

## Precision $\gamma$ -ray branching ratio measurements for long-lived fission products of importance to nuclear-security applications

M. Bencomo,<sup>1</sup> K. Kolos,<sup>1</sup> J.A. Clark,<sup>2</sup> J.C. Hardy,<sup>3</sup> V.E. Iacob,<sup>3</sup> D. Melconian,<sup>3</sup> E. Norman,<sup>4</sup>  
H.I. Park,<sup>3</sup> G. Savard,<sup>2</sup> N.D. Scielzo,<sup>1</sup> and M.A. Stoyer<sup>1</sup>

<sup>1</sup>*Lawrence Livermore National Laboratory*

<sup>2</sup>*Argonne National Laboratory*

<sup>3</sup>*Texas A&M university, College Station, Texas*

<sup>4</sup>*University of California Berkeley, Berkeley, California*

The <sup>95</sup>Zr manuscript describing our experimental approach to measure branching ratios of long-lived fission products has been completed and published in NIM A [1]. This article is an important milestone in this effort and will serve as a great reference for future reports describing results obtained with this approach.

In Ref. [2], we reported on the precision measurements of the branching ratios of long-lived <sup>156</sup>Eu, the statistics and timing of the experiments, as well as some filtering of the data, including random coincidences. After removing random coincidences, we look at all gamma rays that are visible in the spectrum. Determining the area of all gamma-ray peaks in the random-coincidence-free spectrum is not only necessary to calculate the gamma-ray branching ratios but combined with the peak areas of the gamma-ray singles spectrum, we are able to determine experimentally the efficiency of the beta detector:

$$\epsilon_{\beta\gamma} = \frac{R_{\beta\gamma}}{R_{\beta}} \quad (1)$$

where  $R_{\beta\gamma}$  is the rate of the beta-gamma coincidences and  $R_{\beta}$  the rate of gamma singles.

To determine the intensities from the gamma-singles spectrum, the room background must be removed properly. In Fig. 1, we show two of the most intense gamma ray peaks, at 723 keV and 811 keV. Both are transitions coming out of the same energy level, the 1966 keV state. The absolute efficiencies for detecting these transitions with beta detector were calculated to be 0.9765(49) and 0.9799(26), respectively.

After obtaining the experimental efficiencies for all high statistics transitions, we can now compare experimental and simulated efficiencies. The SRIM (Stopping and Range of Ions in Matter) calculations have been made to establish the implantation depth of beam in the carbon foil. This is critical for the  $\beta$  efficiency simulations since the ions are not implanted exactly in the middle of the foil. The depth of implantation was determined by considering the highest yield isotopes in the mass chain, which in this case is <sup>156</sup>Nd, <sup>156</sup>Pm, and <sup>156</sup>Sm. These ions are implanted about ~35 nm deep into the 200-

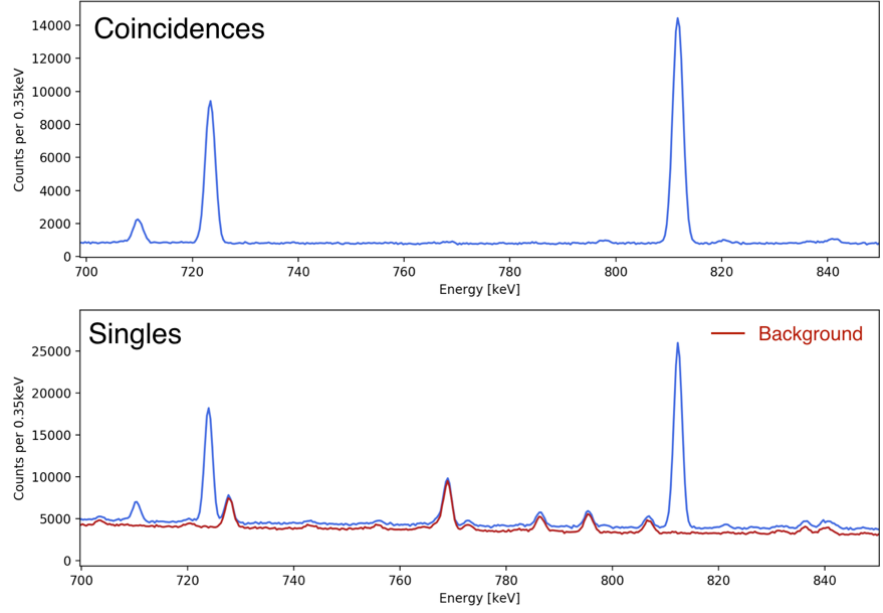


**Fig. 1.** Gamma ray spectra for the region of 700 to 850 keV region, showing two of the most intense gamma-ray transitions, 723 and 811 keV. (Top) Random coincidence free spectrum. (Bottom) Gamma-ray singles spectrum showing the background spectrum used for subtraction.

nm-thick carbon foil (details shown in Fig. 2). We take into consideration the different rates obtained from CARIBU, as well as the slight difference in implantation depth due to the different Z, for each isotope in the mass chain.

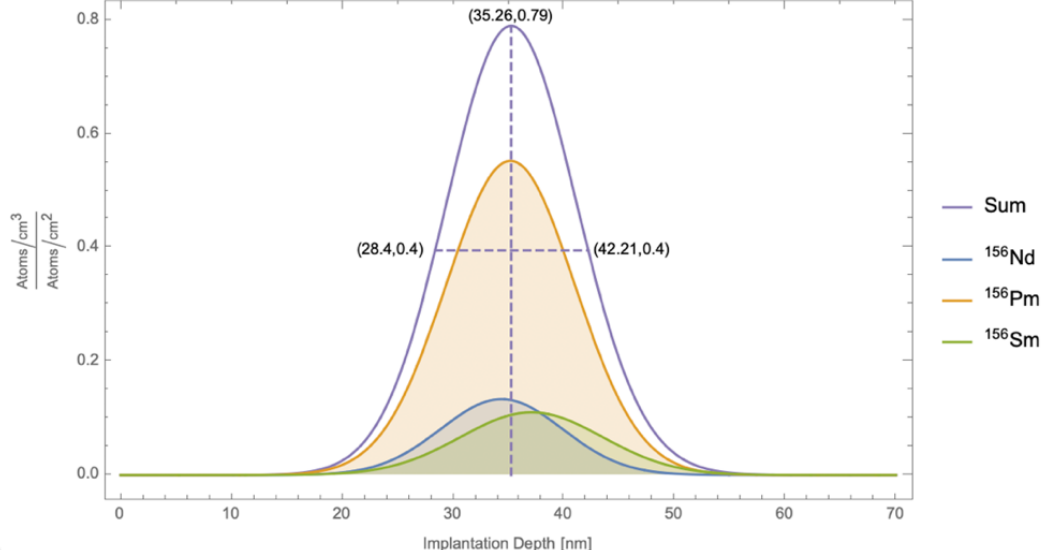


**Fig. 2.** Implantation depth and distribution of the highest yielding isotopes in the mass chain.

Once the implantation depth has been established, it is folded into our simulations. First, a beta decay simulation is performed, giving as a result a variety of particles associated with the decay (beta, gamma, and conversion electrons) including their decay position, energy, and momentum. From this output, we obtain the beta distributions for each transition (see Fig. 3) and use them as input in our GEANT4 model [1] to simulate the response of the gas counter to the different particles associated with the decay. From these simulations we can compare experimental and simulated efficiencies and determine the efficiency of the beta detector.

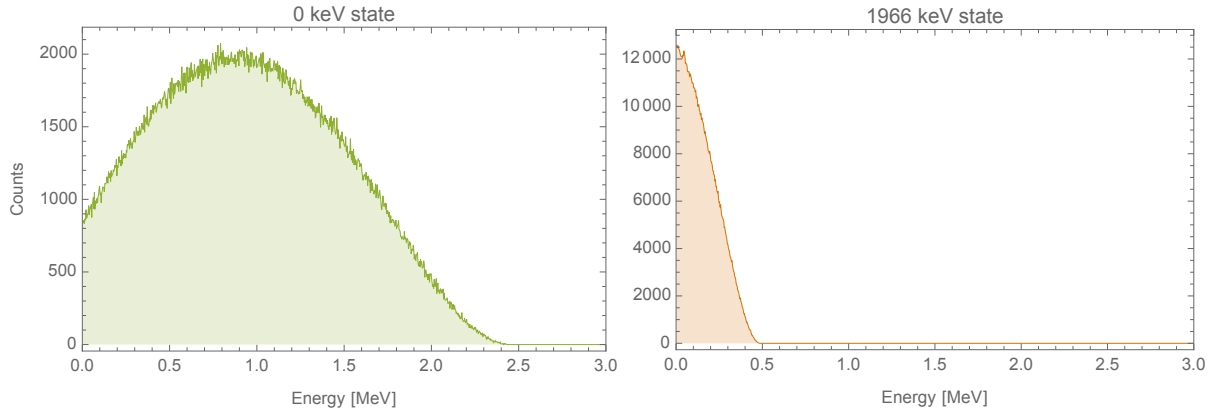


**Fig. 3.** Simulated beta energy distributions for the ground and 1966-keV state in the decay of  $^{156}\text{Eu}$ .

The analysis of the  $^{156}\text{Eu}$  data is not yet finalized but preliminary results show promise for the most intense gamma rays, with uncertainties ranging from 0.3-1.0% so far, we do expect an increase to those uncertainties of about 0.2-0.5%. These results do not include the ratio of the overall beta efficiency,  $\epsilon_\beta$ , to the beta efficiency for a particular transition,  $\epsilon_{\beta i}$  (see Eq. 2), as we have not concluded that part of the analysis but we know that that ratio is very close to unity so the numbers will not change significantly. The other terms for the branching ratio equation have been considered and those are the number of beta-gamma coincidences,  $N_{\beta\gamma}$ , the number of beta singles,  $N_\beta$ , and the efficiency of the germanium detector for a particular energy,  $\epsilon_\gamma$ . Fig. 4 shows a comparison of this work to the current values found in NNDC, the values for our work are listed in Table I with their corresponding uncertainties.

$$BR = \frac{N_{\beta\gamma}}{N_\beta} \frac{1}{\epsilon_\gamma} \frac{\epsilon_\beta}{\epsilon_{\beta i}} \quad (2)$$

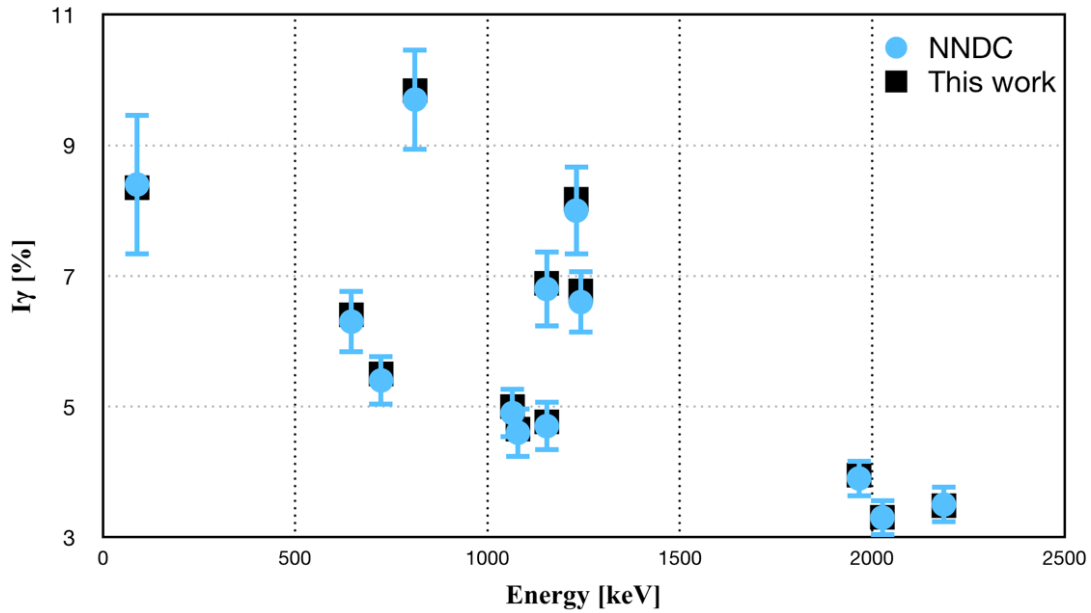


**Fig. 4.** Gamma-ray branching ratio comparison between current values from NNDC (blue dots) and preliminary results from this work (black squares). Error bars for this work are contained within the markers.

**Table I.** Preliminary branching ratios for the 14 most intense gamma rays in the decay of Eu-156.

$\gamma$ -ray energy [keV]	$I_\gamma$ (this work)	$\gamma$ -ray energy [keV]	$I_\gamma$ (this work)
88.97	8.352(30)	1153.67	6.887(46)
599.47	2.135(19)	1154.08	4.755(44)
646.29	6.405(33)	1230.71	8.174(43)
723.47	5.500(31)	1242.42	6.770(38)
811.77	9.837(46)	1965.95	3.949(36)
1065.14	5.000(32)	2026.65	3.305(32)
1079.16	4.655(31)	2186.71	3.483(33)

This work was performed under the auspices of the US Department of Energy (DOE) by the Lawrence Livermore National Laboratory (LLNL) under Contract No. DE-AC52-07NA27344, DE-AC02-06CH11357 (ANL), and DE-FG03-93ER40773 (TAMU), and the University of California under Contract No. DE-AC0376SF0098. This work was supported by the US DOE National Nuclear Security Administration through the Office of Nonproliferation Research and Development (NA-22) under the Funding Opportunity Announcement LAB 17-1763.

[1] K. Kolos, A.M. Hennessy, N.D. Scielzo, V.E. Iacob, J.C. Hardy, M.A. Stoyer, A.P. Tonchev, W.-J. Ong, M.T. Burkey, B. Champine, J.A. Clark, P. Copp, A. Gallant, E.B. Norman, R. Orford, H.I. Park,

J. Rohrer, D. Santiago-Gonzalez, G. Savard, A.J. Shaka, B.S. Wang, and S. Zhu, Nucl. Instrum. Methods Phys. Res. **A1000**, 165240 (2021).

[2] M. Bencomo *et. al.*, *Progress in Research*, Cyclotron Institute, Texas A&M University (2019-2020), p. IV-105.